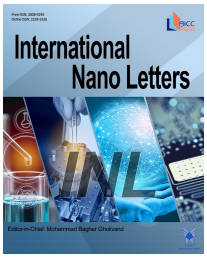

Volume 14, Issue 1, 142401 (1-12)

International Nano Letters (INL)

https://doi.org/10.57647/inl.2024.1401.01

Designing and Optimizing Bioactive Bone Dressing for Tooth Socket Preservation and Regenerative Dentistry Application: In Vitro Study

Elahe Houshmand[1], Sadaf Javadpour[2], Mohammadhossein Ehsani[3], Mike Sabeti[4], Javad Mehrani Sabet[5,**], Seyyed Behnam Abdollahi Boraei[2], Sattar Yousefi[6], Behzad Houshmand[7,*]

[1]*Department of Electronics, Information and Bioengineering, Politecnico di Milano, Milan, Italy.*
[2]*Department of Life Science Engineering, Faculty of New Science and Technologies, University of Tehran, Tehran, Iran.*
[3]*Department of Material Science and Engineering, Sharif University of Technology, Tehran, Iran.*
[4]*School of Dentistry, University of Southern California, Los Angeles, CA, USA.*
[5]*Department of Periodontics, Dental Faculty, Mazandaran University of Medical Sciences, Sari, Iran.*
[6]*Tehran University of Medical Science, Tehran, Iran.*
[7]*Department of Periodontology, Dental School, Shahid Beheshti University of Medical Sciences, Tehran, Iran.*

[*]**Corresponding author:** houshmandperio@gmail.com
[**]**Co-Corresponding author:** dr.j.mehrani.s@gmail.com

Original Research

Received:
8 November 2023
Revised:
20 January 2024
Accepted:
28 February 2024
Published online:
30 March 2024

Abstract:

To address the challenge of preserving sufficient alveolar bone volume and quality following tooth extraction, this in vitro study presents the design and optimization of a bioactive scaffold composed of carboxymethyl cellulose (CMC), alginate (Alg), and tricalcium phosphate (TCP). This composite aims to facilitate post-extraction socket healing and promote osteogenesis. The scaffold was fabricated using freeze-drying to achieve a porous, sponge-like structure. Sodium alginate and CMC were mixed at a 30:70 ratio, with TCP incorporated at 3% wt% and crosslinked using a 0.5 M calcium chloride solution. The formulation was subjected to controlled freezing and lyophilization steps to enhance porosity and mechanical integrity. Characterization studies confirmed a highly porous structure (79% porosity) with interconnected pores, as visualized by SEM. Mechanical testing revealed improved compressive strength due to TCP incorporation, while FTIR and XRD analyses confirmed polymer bonding and the presence of TCP, respectively. Degradation testing showed a slow initial breakdown followed by accelerated degradation, leading to complete scaffold resorption by day 28. Biological assays, including MTT, Alizarin Red staining, and ALP activity, demonstrated the scaffold's excellent biocompatibility and ability to support cell proliferation, migration, and enhanced calcium deposition. These findings suggest that the scaffold has potential for promoting osteogenesis in vitro, warranting further investigation for its possible application in alveolar bone regeneration.

Keywords: Chitosan sponge, bone tissue engineering, tricalcium Phosphate, extraction socket preservation

Cite this article: Houshmand, E., Javadpour, S., Ehsani, M., Sabeti, M., Mehrani Sabet, J., Abdollahi Boraei, S.B., Yousefi, S., Houshmand, B. Designing and Optimizing Bioactive Bone Dressing for Tooth Socket Preservation and Regenerative Dentistry Application: In Vitro Study. *Int. Nano Lett.* **14**(1), 142401 (2024).

1. Introduction

Each year, a significant number of patients receive implant-supported dental prostheses to replace missing teeth lost due to cancer, trauma, or poor oral hygiene [1]. Diabetes mellitus exacerbates periodontal disease by impairing immune response and promoting chronic inflammation, with hyperglycemia-induced advanced glycation end-products (AGEs) contributing to tissue destruction and more severe disease manifestations [2–4]. Following tooth extraction, natural blood clot formation initiates alveolar bone regener-

ation; however, studies show that when the extraction socket is left untreated, substantial bone resorption can occur, limiting the ability to place implants successfully [5, 6]. A critical challenge in implant dentistry is achieving sufficient bone height and width for long-term implant stability [7, 8], and it is estimated that more than 60% of implant sites require some form of bone augmentation to ensure adequate bone volume and quality [9–13].

Immediate implant placement has been proposed to limit post-extraction bone resorption and preserve ridge morphology [14]; however, it does not prevent buccal bone remodeling, particularly in fresh extraction sites [6]. While implant placement itself cannot halt the biological changes following extraction, biomaterials have been suggested as a method to slow down resorption and promote new bone formation. Socket preservation techniques using bone grafts or guided tissue regeneration are commonly performed immediately after extraction to mitigate bone loss [15–18]. A variety of graft materials have been used, including autografts [19, 20], freeze-dried allografts and xenografts [21–24], each with benefits and limitations. Autografts are considered the "gold standard" due to their osteoconductivity, osteoinductivity, and viable osteogenic cells [19], reducing the risk of immune rejection or disease transmission. However, they are associated with donor site morbidity, potential pain, infection, and cosmetic issues [25–30].

To overcome these drawbacks, allografts, xenografts, and, more recently, synthetic or composite materials have been explored. Deproteinized bovine bone (Bio-Oss®, Geistlich Pharma AG, Wolhusen, Switzerland) has shown positive outcomes in clinical and experimental studies, serving as an osteoconductive scaffold for bone regeneration [31–33]. Most synthetic graft materials are based on calcium phosphate ceramics such as β-tricalcium phosphate (β-TCP) and hydroxyapatite, which resemble bone mineral and support osteoblast adhesion [34]. However, their slow degradation can hinder full bone regeneration [17, 35], necessitating the development of materials with improved resorption profiles and biological performance.

Hydrogels based on natural polysaccharides such as sodium alginate, carboxymethyl cellulose (CMC), and dextran have gained traction in bone and tissue engineering applications due to their biocompatibility, biodegradability, and ease of processing [36–40]. Porous scaffolds made from these materials offer high water retention, large surface area, and high porosity ($> 90\%$), which are essential for cell migration and nutrient exchange [41, 42]. CMC, in particular, is an anionic, water-soluble, biodegradable polymer known for its hydrophilicity, viscosity-modifying, and pH-responsive swelling behavior [43–48]. It has demonstrated applications in wound healing, drug delivery, and protein transport systems [49–51], and its cell-adhesive matrix can support attachment and proliferation [52–54].

Sodium alginate, a seaweed-derived polysaccharide composed of β-D-mannuronate and α-L-guluronate blocks, forms hydrogels through ionic crosslinking with divalent cations like Ca^{2+} [55]. Although alginate itself lacks intrinsic cell adhesion properties [56]. Its favorable characteristics—such as rapid gelation, good biocompatibility, wound moisture retention, and hemostatic properties—make it a widely used material in dressings and bone regeneration scaffolds [56–64]. When combined with CMC, alginate can form hydrogen-bonded, hybrid hydrogels with improved mechanical and biological performance [65].

Tricalcium phosphate (TCP), a calcium phosphate ceramic, is known for its high biocompatibility and bioactivity, making it suitable for orthopedic and dental applications. TCP supports osteoblast adhesion, binds proteins and growth factors, and is readily resorbed by the body [66–68]. By combining TCP with CMC and alginate, a composite hydrogel scaffold with both hemostatic and osteoconductive properties can be developed.

In this study, we propose a novel bioactive socket dressing as a moldable cone, composed of tricalcium phosphate, alginate, and carboxymethyl cellulose. This composite scaffold is designed for insertion into tooth extraction sockets to stabilize the clot, promote bleeding control, and enhance natural bone healing and regeneration.

2. Method and materials

2.1 Materials

Sodium alginate (biomedical grade), carboxymethyl cellulose (CMC, low viscosity, biomedical grade), calcium chloride dihydrate ($CaCl_2 \cdot 2H_2O$, $\geq 99\%$ purity), and tricalcium phosphate (β-TCP, biomedical grade) were purchased from Sigma-Aldrich (St. Louis, MO, USA) and used without further purification.

2.2 Methods

To prepare the Carboxymethyl cellulose/alginate/tricalcium phosphate scaffold (figure 1), the carboxymethyl cellulose/alginate solution with a concentration of $3-4\%$ wt% was first prepared. In this solution, the ratio of CMC to alginate is 70% to 30%. To make this solution, an alginate solution was first made at a temperature of 60 °C on a stirrer at a speed of 800 rpm. After homogenization, the CMC solution was slowly added to it. After the CMC was completely dissolved in the solution, an amount of 3% wt% compared to the initial concentration of the solution, tricalcium phosphate was added. In the next step, 2% calcium chloride solution with a concentration of 0.5 M is added to crosslink the solution. The solution was placed on the stirrer for 24 hours at a temperature of 50 °C and a speed of 600 rpm. Before the freeze-drying process, the solution was placed in an ultrasonic device with a power of 50 watts for 10 minutes for homogenization. After that, it was poured into the final mold and placed in a freezer at -20 °C for 24 hours, in a freezer at -80 °C for 8 hours, and then in a freeze-drier for Lyophilization for 48 hours.

2.3 Characterization

2.3.1 Scanning electron microscopy (SEM)

The porosity and surface morphology of the CMC/Alg/TCP scaffold were investigated using scanning electron microscopy. A thin layer of gold was applied after vacuum drying and mounting the sample on carbon tapes. Then, an FE-SEM (TE-SCAN, Czech Republic) was used to examine the material.

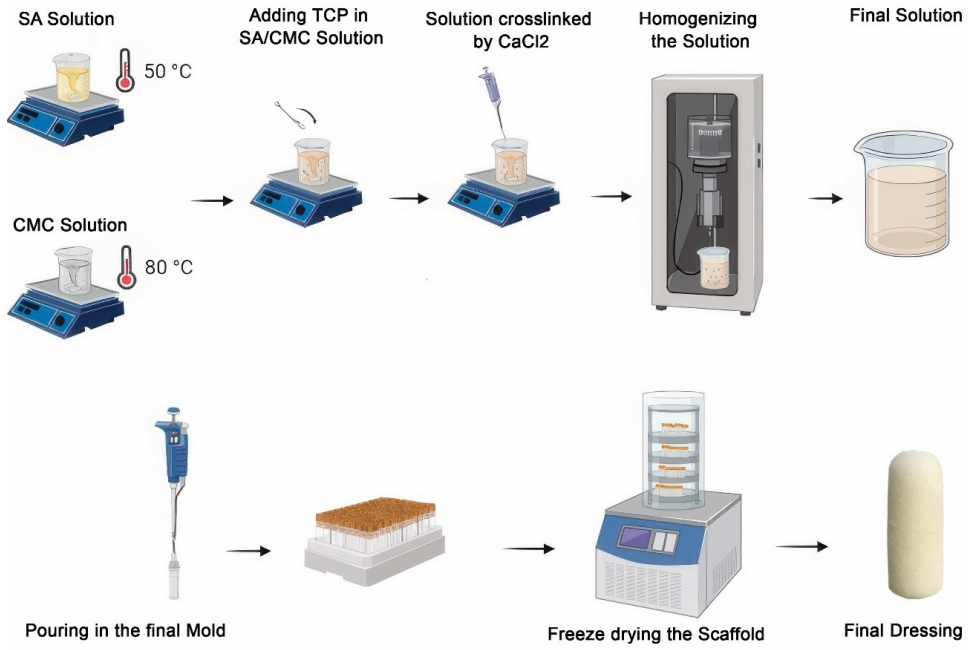

Figure 1. Schematic of preparation of CMC/Alg/TCP bone dressing.

2.3.2 Fourier transform-infrared spectroscopy (FT-IR)

The chemical reactions between the scaffold's constituent parts were characterized using the FTIR. The spectra of the CMC/Alg/TCP scaffolds and the individual scaffold components were recorded using an FTIR spectrophotometer (Thermo Scientific Co., USA). The observed spectra fell between 4000 and 600 cm^{-1}.

2.3.3 X-ray diffraction analysis (XRD)

Using a PHILIPS (Netherlands) X-ray diffractometer with Cu Ka radiation and a scanning rate of one second per step, scaffold X-ray diffraction (XRD) patterns were produced. The X-ray tube has a voltage of 40 kV and a current of 30 mA. The powdered biocomposite scaffold was studied at two angles of $10-50$.

2.3.4 Mechanical testing

Using a load cell of 250 N, cylinder pieces with a 2:1 L/D ratio were mechanically compressed and evaluated on a Universal Testing Machine (SANTAM, Iran). Around 2 mm/min, the crossing-head rate was maintained constant. The samples were loaded up until a 50% deformation was achieved. The tests were run three times, and the average outcomes were shared.

2.3.5 Porosity measurement

The fluid displacement approach was used to calculate the porosity [69]. In summary, the sample was soaked in dehydrated alcohol for 48 hours until it reached saturation, and the porosity of the mixture was determined using the formula:

$$P = \frac{W_2 - W_1}{\rho V_1}$$

where V_1 is the volume prior to immersion, W_1 and W_2 are the sample's weights before and after immersion, respectively, and ρ is a constant representing the density of dehydrated alcohol. Three scaffold samples were tested in parallel.

2.3.6 Degradation rate

According to ISO 10993-13, the degradation test was performed. PBS liquid medium was considered as the most similar liquid to the non-protein part of body fluids. In this test, the sample was immersed entirely in PBS according to the standard, and in an incubator, at 37 °C. The Sample was weighed once before the immersion and once after 1, 3, 7, 14, and 28 days. At the end of each time, the PBS was removed entirely, and the sample was dehydrated. The weight of each sample at that time point relative to its initial weight was recorded against the time of immersion (weight loss).

2.3.7 Cell culture

In DMEM containing 10% fetal bovine serum, 1% penicillin-streptomycin, 0.25 mg/mL fungizone, and 2 mM L-glutamine, osteoblast cell lines (G292) were grown. Cultures were kept alive by replacing the culture media every two days and keeping them at 37 °C with 5% CO_2. For confluency (80%), the culture media were replaced every 48 hours. The following stage made use of the second passage of cells.

2.3.8 MTT assay

The ISO 10993-5 standard was followed in the extraction process to examine the samples' toxicity and their impact on cell growth and multiplication. The samples were first sterilized, and then one milliliter of DMEM was added to each sample for every 3 cm^2. After that, the samples were in the culture medium for one, three, and five days. To find out the cell proliferation rate in this study, 100 microliters of culture media and 1×10^4 cells were added to each well of a 96-well cell culture plate. The plate was then incubated

at 37 °C for 24 hours, or until the cells adhered to the bottom. Following confirmation of cell adhesion, the cells' culture medium was removed as much as possible. Then, 90 microliters of the prepared extracts and 10 microliters of FBS were added to each culture well, and the cells were left for a further 24 hours in the vicinity of these concentrations. Subsequently, each well was filled with 0.5 mg/mL of MTT solution, which was then incubated for 4 hours. After four hours, the solution was taken out of the cells, and DMSO was added to dissolve the purple crystals. The plate was shaken for fifteen minutes in order to dissolve the MTT material better. The concentration of the material dissolved in DMSO was then determined with an ELISA reader.

2.3.9 ALP assay

ALP activities were measured to assess the functional activity of the cells on the scaffolds that had been constructed. At specified intervals (3, 7, and 14 days), the ALP activity was assessed to look into the osteogenic differentiation of G292 osteoblast cells. Following the manufacturer's instructions, an ALP assay kit (Delta Darman Part kit, Iran) was used to measure the ALP activity in the supernatant. In short, G-292 cells were precisely plated at a density of 2×10^4 cells/well in 24-well microliter plates. In the wells, scaffold extracts are poured. As negative controls, three wells without scaffolds were utilized. The plates were incubated in warm air with 5% CO_2 for 3, 7, and 14 days at 7 °C. On days 3, 7, and 14, around 15 µL of supernatant was taken out of each well and processed according to the procedure. In short, the sample's ALP hydrolyzed the p-nitrophenyl phosphate (pNPP) to yield the yellow-colored product p-nitrophenol. A microplate reader was used to measure the absorbance at 405 nm, which is directly proportional to the ALP activity and thus the rate of p-nitrophenol synthesis.

2.3.10 Alizarin red staining and quantification

G292s were subjected to alizarin red staining for 14 days in order to look for mineralization. 48-well plates were used to cultivate cells for 24 hours before the culture medium was removed and scaffold extract was applied to each well. After 14 days, the extract was withdrawn, and the cells were then twice-washed with PBS and fixed with 4% formaldehyde for 30 minutes at 4 °C. After extensive washing three times with PBS to remove non-specific stains or actual deposits of calcified nodules, the cells were stained for 5 minutes with Alizarin Red S solution 0.2% (pH 4.2) and photographed under a microscope. The blot was solubilized with 10% cetylpyridinium chloride monohydrate in 0.1 M PBS (pH 7.0) with shaking for 15 minutes after being washed with dH_2O. The amount of calcium deposition was then measured by measuring the absorbance at 570 nm using an ELISA reader.

3. Result and discussion

3.1 SEM and porosity analysis

Based on the SEM images, the scaffolds have a porous structure with each other. The pore size of the scaffolds is approximately 70 to 150 micrometers with 79% porosity. As seen in figure 2, the connection of the pores is very consistent, which significantly affects cell proliferation [70].

3.2 Characterization of functional groups by FTIR

The FTIR–ATR spectra obtained for the CMC/Alg scaffold, alginate, and carboxymethylcellulose are displayed in Fig. 3. The absorption bands located at 1030 cm^{-1} and 950 cm^{-1} in Fig. 3 (a) signify the stretching of C-H from uronic acid and C-O-C from the glycosidic bond. The stretching vibration of the asymmetric -COO group is represented by the absorption bands at 1600 cm^{-1}, whereas the symmetric -COO group from the carboxylic group is visible at 1416 cm^{-1} and 1290 cm^{-1}. The O-H group is indicated by a broad absorption band visible in the 3200–3500 cm^{-1} area. The O-H group is present in Fig. 3 (b) as evidenced by the broad absorption peak at $3200 - 3500$ cm^{-1}, the stretch vibration of C–H stretching is shown at 2880 cm^{-1}, the C=O stretching is shown at 1600 cm^{-1} by the sharp absorp-

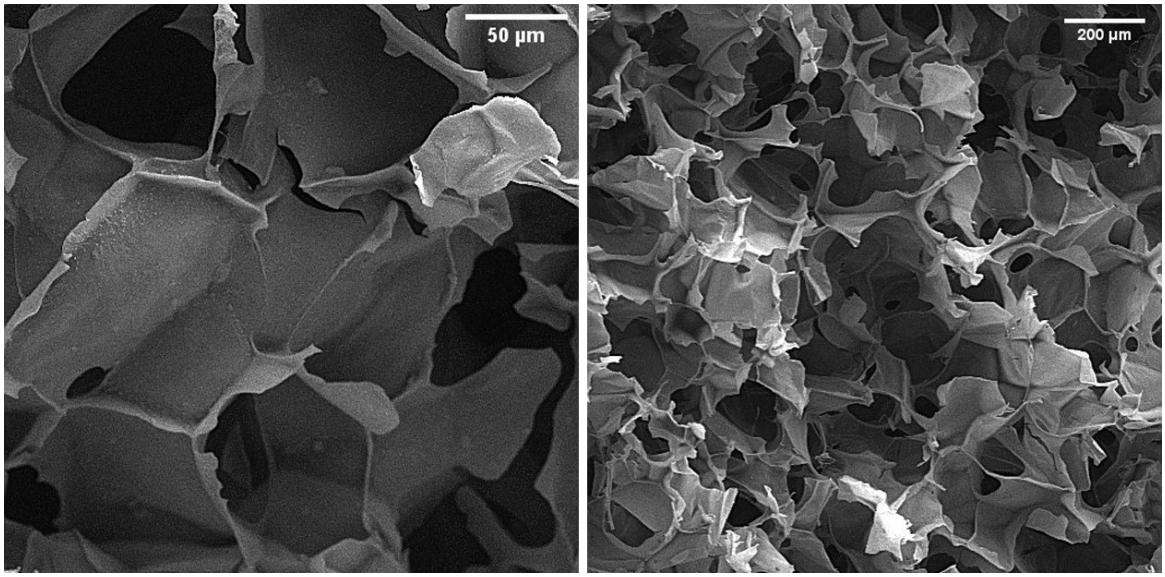

Figure 2. SEM images of carboxymethyl cellulose/alginate/tricalcium phosphate scaffold.

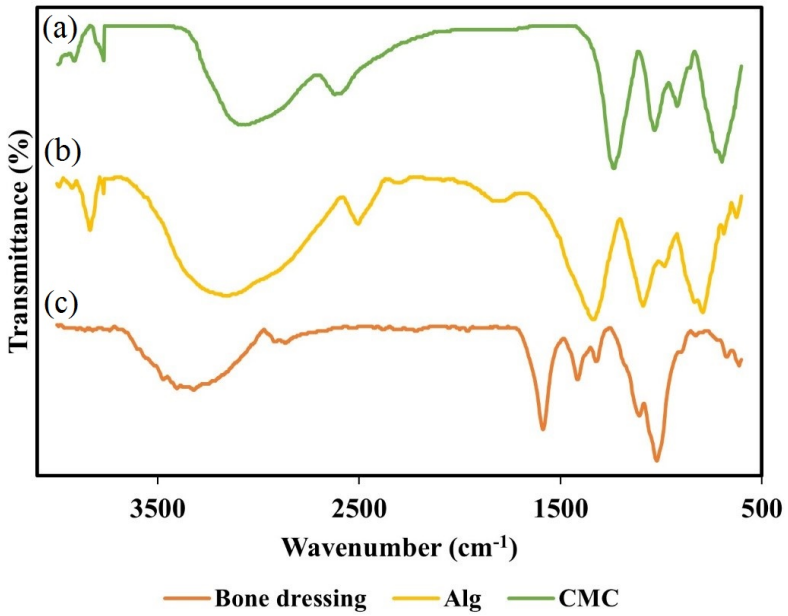

Figure 3. Chemical structure of (a) Alginate, (b) Carboxymethyl cellulose, and (c) CMC/Alg/TCP.

tion band, the scissoring of C–H2 is shown at 1420 cm^{-1}, and the ether group vibration is shown at 1046 cm^{-1}. The peaks for scaffold were found to be slightly displaced to 2864 cm^{-1} from their original locations at 2900 cm^{-1} in both the alginate and CMC peaks, as shown in Fig. 3 (c). The –OH peak (3300 cm^{-1}) in the scaffold moved to 3319 cm^{-1}. These findings could indicate a potential relationship between CMC and Alg in the current study.

3.3 Mechanical properties

A universal testing machine was used to assess the compressive strengths of Alg, CMC, and CMC/Alg/TCP scaffold under 50% compression. Figure 4 illustrates that at the 50% strain zone, the compressive strength of the CMC/Alg/TCP plug (0.142 MPa) was the highest, followed by the Alginate plug (0.098 MPa) and the CMC (0.124 MPa). The CMC/Alg/TCP plug's compressive strength was noticeably higher. The presence of TCP may boost the strength of CMC/Alg/TCP.

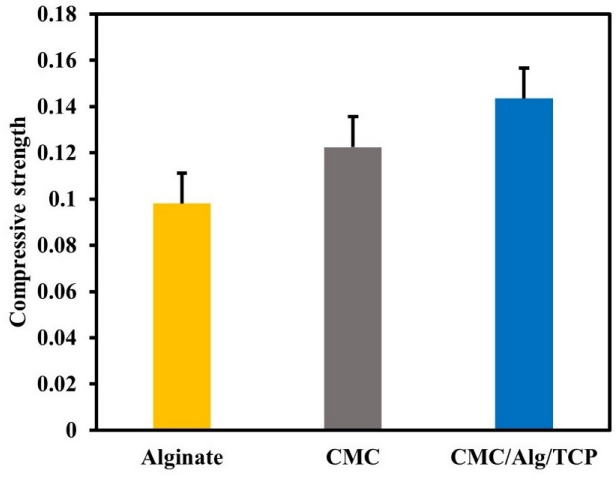

Figure 4. Mechanical strength and modulus of alginate scaffolds, CMC and cross-linked CMC/Alg/TCP dressing.

3.4 X-ray diffraction analysis

XRD examination was conducted to verify the existence of the crystalline phases of β-TCP. The JCPDS two firm diffraction peaks in the β-TCP powder's XRD patterns are located at $2\theta = 25°–32°$, and they correlate to the (2 1 1) and (3 0 0) crystal planes, respectively. Regardless of their polymeric composition, the XRD patterns of the scaffold containing β-TCP likewise showed the peaks correlating with this ceramic, indicating that the ceramic component is present in the scaffold structure (Fig. 5).

3.5 Degradation rate

The rate of degradation was evaluated as it affects the success of the defect repair. This study assessed the degradation of CMC/Alg/TCP bone dressing in PBS solution. The evaluation method was performed by measuring the weight loss of the membrane after leaving it in the PBS solution and drying it at room temperature, respectively, over 28 days. Figure 6 shows the CMC/Alg/TCP scaffold degradation curve over 28 days of testing. The rate of degradation is slow in the first few days and up until the 14^{th} day, which is the useful period for establishing a site and osteogenesis at the tooth site. After that, this rate rises until the 28^{th} day, at which point it is destroyed.

3.6 MTT assay

The MTT test revealed the impact of scaffold extracts on cell viability. At the 24-hour mark, the cells near the scaffold displayed a survival rate similar to the control group. Notably, after 72 hours, the cells cultured with the extract showed a significant increase in survival, suggesting that the

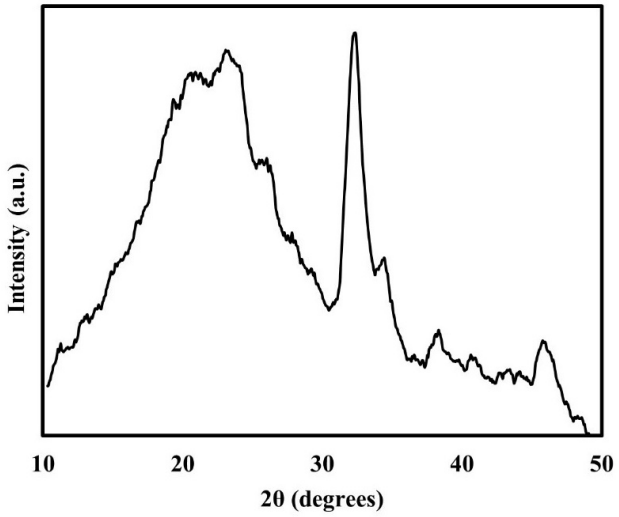

Figure 5. XRD analysis of CMC/Alg/TCP scaffold.

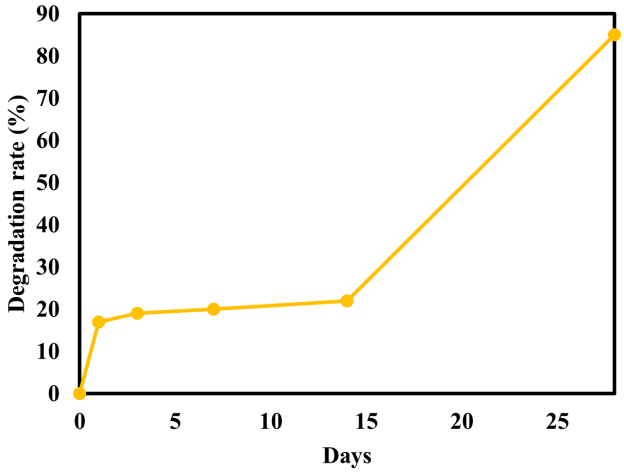

Figure 6. Scaffold degradation rate curve in 28 days.

scaffold aids in bone cell growth and proliferation. However, on the fifth day, the proliferation of G292 cells decreased (Fig. 7). This decline in proliferation could be attributed to an escalation in cell density, leading to the inhibition of intercellular contacts [71].

3.7 ALP assay

The ALP activity was assessed at 3, 7, and 14 days of culture, with normalization based on the respective protein content of each sample. Figure 8 illustrates no notable disparity in ALP activity between the cells exposed to the scaffold and the control group on days 3 and 7. However, the scaffold-exposed cells exhibited higher ALP activity. On the 14th day, a significant difference was observed between the treatment and control groups, indicating the scaffold's positive impact on ALP activity.

3.8 Alizarin red and quantification

Alizarin red S staining was carried out for 14 days to verify calcium's presence in the scaffold throughout cell culture. Figure 9 displays the results of the Alizarin Red S staining. After 14 days, the staining color of the scaffold-cultured

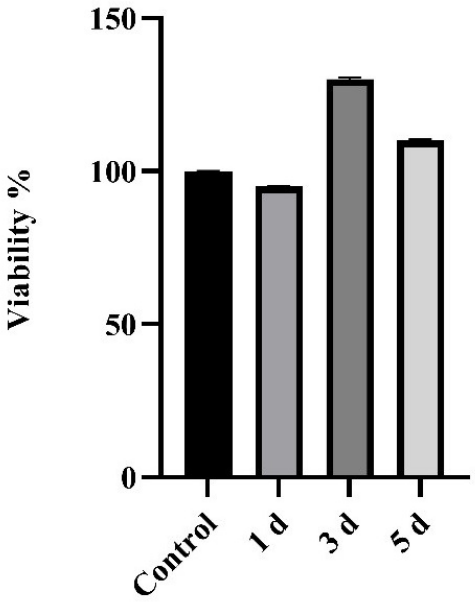

Figure 7. Cell biocompatibility of CMC/Alg/TCP Scaffold, evaluated by MTT assay.

cells grew slightly richer than that of the control group, causing the cells to turn red. The amount of calcium deposition in the scaffold groups was notably larger than in the control group, indicating the scaffold's capacity for osteogenesis. The application of extract treatment led to a notable reduction in extracellular calcium deposition, as seen by the accumulation of mineralized matrix deposition (Fig. 9 (c)).

4. Discussion

The goal of the current investigation was to determine whether CMC/Alg/TCP scaffolds might be used as biomimetic bone dressings to encourage bone repair. Through an SEM study of the scaffolds' surface shape and porosity, it was possible to identify favorable properties for promoting cell adhesion and proliferation. These results are in line with earlier research that showed how crucial the

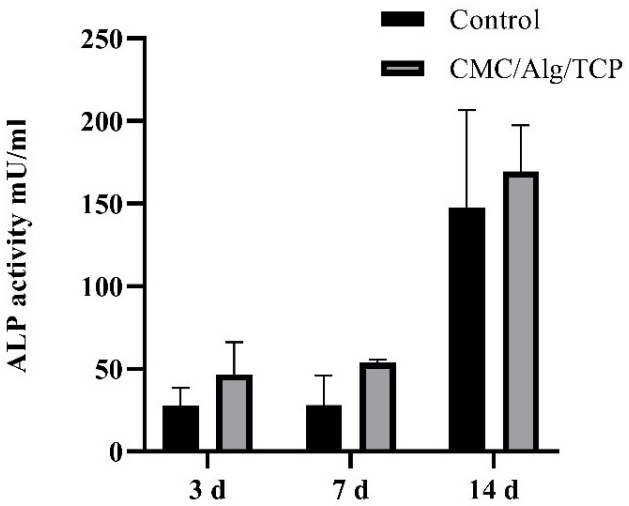

Figure 8. Alkaline phosphatase (ALP) activity by ALP Assay Kit on days 3, 7, and 21 (n = 3 for each group).

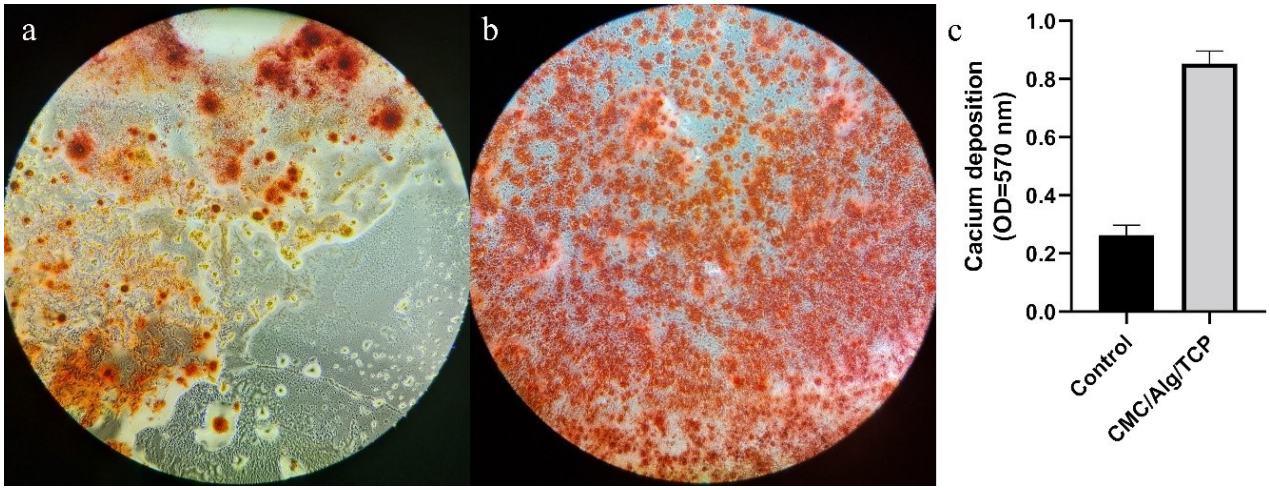

Figure 9. The extracellular calcium deposition was visualized by Alizarin Red S stain after the cells were cultured in the above extracts for 14 days, (a) control group, (b) extract group. Quantification of Alizarin Red staining showing calcium deposition in 14 days.

scaffold microstructure is for promoting tissue regeneration [29]. The CMC/Alg/TCP scaffolds' linked porosity points to the possibility of appropriate cell infiltration and nutrient exchange, both of which are necessary for effective bone regeneration [30].

The CMC/Alg/TCP scaffolds' FTIR examination revealed intermolecular interactions, which suggested that the scaffold's components had been successfully integrated. Given that it offers the requisite cues for cell communication and gene expression, this trait is essential for fostering osteogenic differentiation [72].

Scaffolds' mechanical qualities also significantly affect how well they work. The CMC/Alg/TCP scaffolds tested mechanically showed they could tolerate compressive forces up to 50% distortion. This shows the scaffold's capacity to offer stability and mechanical support during bone regeneration, which is crucial for successful tissue engineering [73].

In this investigation, the effects of the scaffold extract on cell viability, osteogenic differentiation, and mineralization were assessed using the MTT assay, ALP activity evaluation, and Alizarin Red staining, respectively.

Additionally, MTT results revealed that CMC/Alg/TCP scaffolds improved cell viability in comparison, which is consistent with earlier research showing that biodegradable materials, at a particular concentration range, stimulated cell proliferation [74, 75].

An ALP assay was used to evaluate the ALP activity, a marker of early osteogenic differentiation, at various time points (3, 7, and 14 days). On days 3 and 7, the findings revealed no appreciable difference in the ALP activity between the scaffold-exposed and control cells. The scaffold-exposed cells did, however, display increased ALP activity on day 14, indicating improved osteogenic differentiation. According to this research, the scaffold extract encourages G292 cells to differentiate into osteoblasts, which are essential for bone regrowth.

To measure mineralization, G292 cells were stained with Alizarin Red for 14 days. 48-well plates of cells were used for culture, and scaffold extract was applied. The cells were fixed, cleaned, and stained with Alizarin Red S solution after 14 days. Compared to the control group, the stained cells had a deeper red hue, indicating increased calcium deposition and probable mineralization in the scaffold-exposed cells. Moreover, the quantitative data on Alizarin Red staining determines the mineralization extent, demonstrating that this scaffold can enhance the calcium deposition. Based on the results, we proposed several concepts in Table 1.

A future research roadmap in the realm of dental implantology explores optimizing bio-scaffold development via innovative technologies and materials, conducting advanced analytical and cellular studies, executing detailed in vivo and clinical trials, enhancing biodegradability and drug delivery, ensuring scalable production, regulatory compliance, and fostering global collaboration and knowledge dissemination to facilitate bone regeneration post-tooth extraction. Based on that, the Future Research Roadmap can be explained in 8 phases mentioned in Table 2.

While the current findings highlight the promising potential of the CMC/Alg/TCP composite dressing in promoting socket preservation and supporting bone regeneration, several aspects require further investigation before clinical translation can be recommended.

The comprehensive in vivo studies in small animal models are necessary to evaluate the material's biological performance in a dynamic oral environment. Factors such as local inflammation, salivary enzymes, and mechanical loading may affect the degradation profile, hemostatic function, and osteoconductive capacity of the dressing. Additionally, long-term studies are essential to determine the rate of scaffold resorption, the quality and volume of newly formed bone, and the stability of subsequent implant placement.

In conclusion, although the presented CMC/Alg/TCP composite scaffold demonstrates strong potential as a socket preservation dressing, systematic preclinical and clinical evaluations are indispensable to ensure its safety, efficacy, and practical applicability in dental implantology.

Table 1. Concepts, explanation, and highlights based on the result.

Concepts	Brief Explanation	Highlighting
Scaffold Structural Efficacy	Emphasis on porous structure and its effect on cell proliferation	Highlight the observed porous structure and its potential implication for enhancing cell proliferation, given that the consistent pore connections have been indicated to impact this aspect notably.
Functional Group Characterization and Compatibility	Explanation regarding active groups and FTIR results	Emphasize the significance of the identified functional groups in alginate and CMC, and how the FTIR results demonstrate successful integration and potential interaction in the CMC/Alg scaffold.
Mechanical Strength	Analysis and discussion on compressive strengths of the structures	The comparative analysis of the compressive strengths of Alg, CMC, and CMC/Alg/TCP scaffold emphasizes the latter's superior mechanical properties and its implications for durability and resilience in a potential in vivo setting.
Crystalline Phase Confirmation	Confirming the presence of β-TCP crystal phases	Validate the crystalline phases of β-TCP and their persistence within the scaffold, ensuring that the ceramic component, vital for osteoconduction, remains integral in the structure.
Controlled Degradation	Examining the controlled degradation rate of the scaffold	Affirm the controlled degradation rate as pivotal for allowing enough time for osteogenesis at the defect site while ensuring eventual scaffold breakdown.
Cell Viability and Proliferation	Analysis of MTT assay results and their impact on cell growth	Discuss the MTT assay results, pointing out that while the scaffold appears to be biocompatible and initially promotes cell survival and proliferation, the longer-term viability might be influenced by factors like cell density.
Osteogenic Potential	Emphasizing ALP activity and calcium deposition	Highlight the positive impact on ALP activity and calcium deposition, indicating the scaffold's potential to facilitate osteogenesis.
Calcium Deposition and Osteogenesis Ability	Investigating results from Alizarin Red S staining	Discuss the outcomes of the Alizarin Red S staining, recognizing the scaffold's capacity to not only host cells but to possibly influence calcified matrix deposition and thereby support the osteogenic process.
Possible Improvements and Further Research	Suggestions for optimization and future investigations	Introduce the need for further studies to optimize scaffold properties, investigate longer-term in vitro outcomes, and potentially explore in vivo implications. Consider discussing any inconsistencies or unexpected findings, such as the decline in cell proliferation over time, and speculate on the underlying reasons while suggesting avenues for future research.
Clinical Implications	Elucidating potential clinical applications considering the findings	Discuss the potential implications of your conclusions for clinical applications, considering the scaffold's effectiveness in providing a suitable environment for cell growth and proliferation, its mechanical strength, and its biodegradation profile.

Table 2. Future research roadmap.

Phase	Title	Key Activities and Focus Areas
1	Augmentation of Biodegradable Scaffold Development	Hybrid scaffold development, 3D bioprinting, incorporation of growth factors
2	Advanced Analytical Techniques	Application of nanotechnology, in-depth FTIR, and mechanical property analysis
3	Cellular and Molecular Dynamics	Investigate cell-matrix interactions, delve into stem cell research, and analyze genetic expressions related to osteogenesis.
4	Real-time In Vivo Studies	Implement live imaging technologies and explore immunological responses in the host.
5	Biodegradability and Drug Delivery System Enhancement	Develop controlled drug delivery systems, investigate means for temporal control of biodegradability
6	Clinical Studies and Application	Conduct rigorous preclinical and human clinical trials, adhering to ethical considerations and robust data collection methodologies
7	Commercialization and Policy-Making	Strategies for scalable production, ensuring regulatory compliance, and engaging in policy development
8	Continuous Improvement and Knowledge Dissemination	Employ feedback for methodological optimization, foster global collaborations, and initiate education and training programs for professionals

5. Conclusion

In conclusion, the research underscores the promising potential of CMC/Alg/TCP scaffolds in promoting bone repair and regeneration, particularly following tooth extraction. The scaffold exhibited favorable porosity, mechanical strength, and biocompatibility, critical for cell adhesion, proliferation, and nutrient exchange, pivotal for effective bone regeneration. FTIR analysis affirmed successful integration of the scaffold's components, while mechanical tests proved its capability to provide crucial stability and mechanical support during bone regeneration. Moreover, biological evaluations, including the MTT assay, ALP activity, and Alizarin Red staining, revealed the scaffold's positive influence on cell viability, osteogenic differentiation, and mineralization. Thus, the CMC/Alg/TCP scaffold enhances cell viability and osteogenic differentiation and supports mineralization, showcasing its significant potential as a biomimetic bone dressing to foster bone repair. It is a noteworthy subject for further research and potential clinical applications.

Acknowledgments
The authors would like to express their gratitude to all those who indirectly contributed to this work.

Ethical Approval
This study was conducted without the involvement of human or animal subjects, thereby eliminating the need for ethical approval related to human or animal testing. The research focused on the in vitro development, fabrication, and characterization of a composite scaffold composed of carboxymethyl cellulose (CMC), alginate (Alg), and tricalcium phosphate (TCP), intended for use in alveolar bone regeneration following tooth extraction. All materials utilized in the study were sourced from reputable suppliers and were used according to safety guidelines. The absence of direct interaction with living subjects underscores the study's commitment to ethical research practices while contributing valuable insights into biomaterials for medical applications.

Authors Contribution
Each author has made meaningful contributions to the development and completion of this research. Their individual roles are outlined below:
Elahe Houshmand contributed to the initial drafting of the manuscript, played a key role in data interpretation, and was actively involved in study coordination. Sadaf Javadpour played a key role in designing the study and offered valuable revisions during manuscript preparation. Mohammadhossein Ehsani provided critical feedback on the manuscript and supported data collection efforts. Mike Sbeti contributed to the study's conception and design and offered guidance on data analysis and interpretation. Javad Mehrani contributed to data analysis and interpretation and supported manuscript development. Seyyed Behnam Abdollahi Boraei reviewed and offered substantial revisions to the manuscript. Sattar Yousefi was involved in data collection and analysis and assisted with manuscript revision. Behzad Houshmand was involved in conceiving the study, assisted with coordination, and reviewed the manuscript while participating in critical manuscript editing.
All authors have read and approved the final version of the manuscript. We affirm that each has made significant contributions to the study and ensured the accuracy and integrity of the final work.

Availability of data and materials
The datasets generated during and/or analyzed during the current study are available from the corresponding author on reasonable request.

Conflict of interests
The authors declare that they have no known competing financial interests or personal relationships that could have appeared to influence the work reported in this paper.

References

[1] A. Brown, S. Zaky, H. Ray Jr, and C. Sfeir. Porous magnesium/PLGA composite scaffolds for enhanced bone regeneration following tooth extraction. *Acta Biomaterialia*, **11**:543–553, (2015). DOI: https://doi.org/10.1016/j.actbio.2014.09.008.

[2] G. W. Taylor. Bidirectional interrelationships between diabetes and periodontal diseases: An epidemiologic perspective. *Annals of Periodontology*, **6**(1):99–112, (2001). DOI: https://doi.org/10.1902/annals.2001.6.1.99.

[3] B. L. Mealey and T. W. Oates. Diabetes mellitus and periodontal diseases. *Journal of Periodontology*, **77**(8):1289–1303, (2006). DOI: https://doi.org/10.1902/jop.2006.050459.

[4] P. M. Preshaw, A. L. Alba, D. Herrera, S. Jepsen, A. Konstantinidis, K. Makrilakis, and R. Taylor. Periodontitis and diabetes: a two-way relationship. *Diabetologia*, **55**(1):21–31, (2012). DOI: https://doi.org/10.1007/s00125-011-2342-y.

[5] J. Pietrokovski and M. Massler. Alveolar ridge resorption following tooth extraction. *Journal of Prosthetic Dentistry*, **17**(1):21–27, (1967). DOI: https://doi.org/10.1016/0022-3913(67)90046-7.

[6] M.G. Araújo and J. Lindhe. Dimensional ridge alterations following tooth extraction. An experimental study in the dog. *Journal of Clinical Periodontology*, **32**(2):212–218, (2005). DOI: https://doi.org/10.1111/j.1600-051X.2005.00642.x.

[7] D. Buser, K. Dula, H. P. Hirt, and R. K. Schenk. Lateral ridge augmentation using autografts and barrier membranes: A clinical study with 40 partially edentulous patients. *Journal of Oral and Maxillofacial Surgery*, **54**(4):420–432, (1996). DOI: https://doi.org/10.1016/s0278-2391(96)90113-5.

[8] P. M. Camargo, V. Lekovic, M. Weinlaender, P. R. Klokkevold, E. B. Kenney, B. Dimitrijevic, M. Nedic, S. Jancovic, and M. Orsini. Influence of bioactive glass on changes in alveolar process dimensions after exodontia. *Oral Surgery, Oral Medicine, Oral Pathology, Oral Radiology, and Endodontology*, **90**(5):581–586, (2000). DOI: https://doi.org/10.1067/moe.2000.110035.

[9] P. Proussaefs and J. Lozada. The use of intraorally harvested autogenous block grafts for vertical alveolar ridge augmentation: A human study. *International Journal of Periodontics & Restorative Dentistry*, **25**(4), (2005).

[10] S. S. Wallace, S. J. Froum, N. Elian, D. Monteiro, and D. P. Tarnow. Sinus augmentation utilizing anorganic bovine bone (Bio-Oss) with absorbable and nonabsorbable membranes placed over the lateral window: histomorphometric and clinical analyses. *International Journal of Periodontics & Restorative Dentistry*, **25**(6), (2005).

[11] B. S. McAllister and K. Haghighat. Bone augmentation techniques. *Journal of Periodontology*, **78**(3):377–396, (2007). DOI: https://doi.org/10.1902/jop.2007.060048.

[12] S. Fickl, O. Zuhr, H. Wachtel, W. Bolz, and M. B. Huerzeler. Hard tissue alterations after socket preservation: an experimental study in the beagle dog. *Clinical Oral Implants Research*, **19**(11):1111–1118, (2008). DOI: https://doi.org/10.1111/j.1600-0501.2008.01575.x.

[13] J. Ten Heggeler, D. Slot, and G. Van der Weijden. Effect of socket preservation therapies following tooth extraction in non-molar regions in humans: A systematic review. *Clinical oral Implants Research*, **22**(8):779–788, (2011). DOI: https://doi.org/10.1111/j.1600-0501.2010.02064.x.

[14] M. Paolantonio, M. Dolci, A. Scarano, D. d'Archivio, G. Di Placido, V. Tumini, and A. Piattelli. Immediate implantation in fresh extraction sockets. A controlled clinical and histological study in man. *Journal of Periodontology*.

[15] V. Lekovic, P. M. Camargo, P. R. Klokkevold, M. Weinlaender, E. B. Kenney, B. Dimitrijevic, and M. Nedic. Preservation of alveolar bone in extraction sockets using bioabsorbable membranes. *Journal of Periodontology*, **69**(9):1044–1049, (1998). DOI: https://doi.org/10.1902/jop.1998.69.9.1044.

[16] O. Hoffmann, B. K. Bartee, C. Beaumont, A. Kasaj, G. Deli, and G. G. Zafiropoulos. Alveolar bone preservation in extraction sockets using non-resorbable dPTFE membranes: A retrospective non-randomized study. *Journal of Periodontology*, **79**(8):1355–1369, (2008). DOI: https://doi.org/10.1902/jop.2008.070502.

[17] N. Mardas, V. Chadha, and N. Donos. Alveolar ridge preservation with guided bone regeneration and a synthetic bone substitute or a bovine-derived xenograft: A randomized, controlled clinical trial. *Clinical Oral Implants Research*, **21**(7):688–698, (2010). DOI: https://doi.org/10.1111/j.1600-0501.2010.01918.x.

[18] M. Retzepi and N. Donos. Guided bone regeneration: Biological principle and therapeutic applications. *Clinical Oral Implants Research*, **21**(6):567–576, (2010). DOI: https://doi.org/10.1111/j.1600-0501.2010.01922.x.

[19] W. Becker, M. Urist, B. E. Becker, W. Jackson, D. A. Party, M. Bartold, G. Vincenzzi, D. De Georges, and M. Niederwanger. Clinical and histologic observations of sites implanted with intraoral autologous bone grafts or allografts. 15 human case reports. *Journal of Periodontology*.

[20] M. G. Araujo and J. Lindhe. Socket grafting with the use of autologous bone: an experimental study in the dog. . *Clinical Oral Implants Research*, **22**(1):9–13, (2011). DOI: https://doi.org/10.1111/j.1600-0501.2010.01937.x.

[21] J. M. Iasella, H. Greenwell, R. L. Miller, M. Hill, C. Drisko, A. A. Bohra, and J. P. Scheetz. Ridge preservation with freeze-dried bone allograft and a collagen membrane compared to extraction alone for implant site development: A clinical and histologic study in humans. *Journal of Periodontology*, **74**(7):990–999, (2003). DOI: https://doi.org/10.1902/jop.2003.74.7.990.

[22] G. Zubillaga, S. Von Hagen, B. I. Simon, and M. J. Deasy. Changes in alveolar bone height and width following post-extraction ridge augmentation using a fixed bioabsorbable membrane and demineralized freeze-dried bone osteoinductive graft. *Journal of Periodontology*, **74**(7):965–975, (2003). DOI: https://doi.org/10.1902/jop.2003.74.7.965.

[23] C. S. Kim, S. H. Choi, K. S. Cho, J. K. Chai, U. M. Wikesjö, and C. K. Kim. Periodontal healing in one-wall intra-bony defects in dogs following implantation of autogenous bone or a coral-derived biomaterial. *Journal of Clinical Periodontology*, **32**(6):583–589, (2005). DOI: https://doi.org/10.1111/j.1600-051X.2005.00729.x.

[24] G. C. Keles, M. Sumer, B. O. Cetinkaya, F. Tutkun, and S. B. Simsek. Effect of autogenous cortical bone grafting in conjunction with guided tissue regeneration in the treatment of intraosseous periodontal defects. *European Journal of Dentistry*, **4**(04):403–411, (2010).

[25] C. R. Perry. Bone repair techniques, bone graft, and bone graft substitutes. *Clinical Orthopaedics and Related Research®*, **360**: 71–86, (1999). DOI: https://doi.org/10.1097/00003086-199903000-00010.

[26] S. C. Ludwig, J. M. Kowalski, and S. D. Boden. Osteoinductive bone graft substitutes. *European Spine Journal*, **9**(Suppl 1):S119–S125, (2000). DOI: https://doi.org/10.1007/pl00008317.

[27] M. Yildirim, H. Spiekermann, S. Biesterfeld, and D. Edelhoff. Maxillary sinus augmentation using xenogenic bone substitute material Bio-Oss® in combination with venous blood: A histologic and histomorphometric study in humans. . *Clinical Oral Implants Research*, **11**(3):217–229, (2000). DOI: https://doi.org/10.1034/j.1600-0501.2000.011003217.x.

[28] D. Apelt, F. Theiss, A. El-Warrak, K. Zlinszky, R. Bettschart-Wolfisberger, M. Bohner, S. Matter, J. A. Auer, and B. von Rechenberg. In vivo behavior of three different injectable hydraulic calcium phosphate cements. *Biomaterials*, **25**(7-8):1439–1451, (2004). DOI: https://doi.org/10.1016/j.biomaterials.2003.08.073.

[29] P. V. Giannoudis, H. Dinopoulos, and E. Tsiridis. Bone substitutes: An update. *Injury*, **36**(3):S20–S27, (2005). DOI: https://doi.org/10.1016/j.injury.2005.07.029.

[30] F. M. Tamimi, J. Torres, I. Tresguerres, C. Clemente, E. López-Cabarcos, and L. J. Blanco. Bone augmentation in rabbit calvariae: Comparative study between Bio-Oss® and a novel β-TCP/DCPD granulate. *Journal of Clinical Periodontology*.

[31] T. Berglundh and J. Lindhe. Healing around implants placed in bone defects treated with Bio-Oss®. An experimental study in the dog. *Clinical Oral Implants Research*, **8**(2):117–124, (1997). DOI: https://doi.org/10.1034/j.1600-0501.1997.080206.x.

[32] D. Carmagnola, P. Adriaens, and T. Berglundh. Healing of human extraction sockets filled with Bio-Oss®. *Clinical Oral Implants Research*, **14**(2):137–143, (2003). DOI: https://doi.org/10.1034/j.1600-0501.2003.140201.x.

[33] G. Cardaropoli, M. Araújo, R. Hayacibara, F. Sukekava, and J. Lindhe. Healing of extraction sockets and surgically produced–augmented and non-augmented–defects in the alveolar ridge. An experimental study in the dog. *Journal of Clinical Periodontology*, **32**(5):435–440, (2005). DOI: https://doi.org/10.1111/j.1600-051X.2005.00692.x.

[34] R. Z. LeGeros. Properties of osteoconductive biomaterials: Calcium phosphates. *Clinical Orthopaedics and Related Research®*, **395**: 81–98.

[35] J. Frenken, W. Bouwman, N. Bravenboer, S. Zijderveld, E. Schulten, and C. Ten Bruggenkate. The use of Straumann® Bone Ceramic in a maxillary sinus floor elevation procedure: a clinical, radiological, histological and histomorphometric evaluation with a 6-month healing period. *Clinical Oral Implants Research*, **21**(2):201–208, (2010). DOI: https://doi.org/10.1111/j.1600-0501.2009.01821.x.

[36] R. Muzzarelli, V. Baldassarre, F. Conti, P. Ferrara, G. Biagini, G. Gazzanelli, and V. Vasi. Biological activity of chitosan: ultrastructural study. *Biomaterials*, **9**(3):247–252, (1988). DOI: https://doi.org/10.1016/0142-9612(88)90092-0.

[37] J. M. Dang and K. W. Leong. Natural polymers for gene delivery and tissue engineering. *Advanced Drug Delivery Reviews*, **58**(4): 487–499, (2006). DOI: https://doi.org/10.1016/j.addr.2006.03.001.

[38] M. George and T. E. Abraham. Polyionic hydrocolloids for the intestinal delivery of protein drugs: alginate and chitosan—a review. *Journal of Controlled Release*, **114**(1):1–14, (2006). DOI: https://doi.org/10.1016/j.jconrel.2006.04.017.

[39] I.-Y. Kim, S.-J. Seo, H.-S. Moon, M.-K. Yoo, I.-Y. Park, B.-C. Kim, and C.-S. Cho. Chitosan and its derivatives for tissue engineering applications. . *Biotechnology Advances*, **26**(1):1–21, (2008). DOI: https://doi.org/10.1016/j.biotechadv.2007.07.009.

[40] R. Bilgainya, F. Khan, and S. Mann. Spontaneous patterning and nanoparticle encapsulation in carboxymethylcellulose/alginate/dextran hydrogels and sponges. *Materials Science and Engineering: C*, **30**(3):352–356, (2010). DOI: https://doi.org/10.1016/j.msec.2009.11.010.

[41] L. Ma, C. Gao, Z. Mao, J. Zhou, J. Shen, X. Hu, and C. Han. Collagen/chitosan porous scaffolds with improved biostability for skin tissue engineering. *Biomaterials*, **24**(26):4833–4841, (2003). DOI: https://doi.org/10.1016/s0142-9612(03)00374-0.

[42] K. Rezwan, Q. Chen, J. J. Blaker, and A. R. Boccaccini. Biodegradable and bioactive porous polymer/inorganic composite scaffolds for bone tissue engineering. *Biomaterials*.

[43] A. Sannino, C. Demitri, and M. Madaghiele. Biodegradable cellulose-based hydrogels: design and applications. *Materials*, **2**(2):353–373, (2009). DOI: https://doi.org/10.3390/ma2020353.

[44] S. Gorgieva and V. Kokol. Synthesis and application of new temperature-responsive hydrogels based on carboxymethyl and hydroxyethyl cellulose derivatives for the functional finishing of cotton knitwear. *Carbohydrate Polymers*, **85**(3):664–673, (2011). DOI: https://doi.org/10.1016/j.carbpol.2011.03.037.

[45] E. Akar, A. Altınışık, and Y. Seki. Preparation of pH-and ionic-strength responsive biodegradable fumaric acid crosslinked carboxymethyl cellulose. *Carbohydrate Polymers*, **90**(4):1634–1641, (2012). DOI: https://doi.org/10.1016/j.carbpol.2012.07.043.

[46] M. Yadollahi, H. Namazi, and S. Barkhordari. Preparation and properties of carboxymethyl cellulose/layered double hydroxide bionanocomposite films. *Carbohydrate Polymers*, **108**:83–90.

[47] M. Dilaver and K. Yurdakoc. Fumaric acid cross-linked carboxymethylcellulose/poly (vinyl alcohol) hydrogels. *Polymer Bulletin*, **73**(10):2661–2675, (2016). DOI: https://doi.org/10.1007/s00289-016-1613-7.

[48] B. Singh, N. Panda, R. Mund, and K. Pramanik. Carboxymethyl cellulose enables silk fibroin nanofibrous scaffold with enhanced biomimetic potential for bone tissue engineering application. *Carbohydrate Polymers*, **151**:335–347, (2016). DOI: https://doi.org/10.1016/j.carbpol.2016.05.088.

[49] W. J. Zheng, J. Gao, Z. Wei, J. Zhou, and Y. M. Chen. Facile fabrication of self-healing carboxymethyl cellulose hydrogels. *European Polymer Journal*, **72**:514–522, (2015). DOI: https://doi.org/10.3390/gels7040216.

[50] P. Basu, U. Narendrakumar, R. Arunachalam, S. Devi, and I. Manjubala. Characterization and evaluation of carboxymethyl cellulose-based films for healing of full-thickness wounds in normal and diabetic rats. *ACS Omega*, **3**(10):12622–12632, (2018). DOI: https://doi.org/10.1021/acsomega.8b02015.

[51] D. Jeong, S.-W. Joo, Y. Hu, V. V. Shinde, E. Cho, and S. Jung. Carboxymethyl cellulose-based superabsorbent hydrogels containing carboxymehtyl β-cyclodextrin for enhanced mechanical strength and effective drug delivery. *European Polymer Journal*, **105**:17–25, (2018). DOI: https://doi.org/10.1016/j.eurpolymj.2018.05.023.

[52] Q. Garrett, P. A. Simmons, S. Xu, J. Vehige, Z. Zhao, K. Ehrmann, and M. Willcox. Carboxymethylcellulose binds to human corneal epithelial cells and is a modulator of corneal epithelial wound healing. . *Investigative Ophthalmology & Visual Science*, **48**(4):1559–1567, (2007). DOI: https://doi.org/10.1167/iovs.06-0848.

[53] W. Tongdeesoontorn, L. J. Mauer, S. Wongruong, P. Sriburi, and P. Rachtanapun. Effect of carboxymethyl cellulose concentration on physical properties of biodegradable cassava starch-based films. *Chemistry Central Journal*, **5**(1):6, (2011). DOI: https://doi.org/10.1186/1752-153X-5-6.

[54] Y. Han and L. Wang. Sodium alginate/carboxymethyl cellulose films containing pyrogallic acid: physical and antibacterial properties. *Journal of the Science of Food and Agriculture*.

[55] D. Jaikumar, K. Sajesh, S. Soumya, T. Nimal, K. Chennazhi, S. V. Nair, and R. Jayakumar. Injectable alginate-O-carboxymethyl chitosan/nano fibrin composite hydrogels for adipose tissue engineering. *International Journal of Biological Macromolecules*, **74**:318–326, (2015). DOI: https://doi.org/10.1016/j.ijbiomac.2014.12.037.

[56] A. Mellati, E. Hasanzadeh, M. Gholipourmalekabadi, and S. E. Enderami. Injectable nanocomposite hydrogels as an emerging platform for biomedical applications: A review. *Materials Science and Engineering: C*, **131**:112489, (2021).
DOI: https://doi.org/10.1016/j.msec.2021.112489.

[57] T. Billiet, E. Gevaert, T. De Schryver, M. Cornelissen, and P. Dubruel. The 3D printing of gelatin methacrylamide cell-laden tissue-engineered constructs with high cell viability. *Biomaterials*, **35**(1):49–62.

[58] C. Mota, D. Puppi, F. Chiellini, and E. Chiellini. Additive manufacturing techniques for the production of tissue engineering constructs. *Journal of Tissue Engineering and Regenerative Medicine*, **9**(3): 174–190.

[59] T. Kageyama, T. Osaki, J. Enomoto, D. Myasnikova, T. Nittami, T. Hozumi, T. Ito, and J. Fukuda. In situ cross-linkable gelatin-CMC hydrogels designed for rapid engineering of perfusable vasculatures. *ACS Biomaterials Science & Engineering*, **2**(6):1059–1066, (2016).
DOI: https://doi.org/10.1021/acsbiomaterials.6b00203.

[60] T. Maver, D. Smrke, M. Kurečič, L. Gradišnik, U. Maver, and K. S. Kleinschek. Combining 3D printing and electrospinning for preparation of pain-relieving wound-dressing materials. *Journal of Sol-Gel Science and Technology*, **88**(1):33–48, (2018).
DOI: https://doi.org/10.1007/s10971-018-4630-1.

[61] Y. Chen, H. Qiu, M. Dong, B. Cheng, Y. Jin, Z. Tong, P. Li, S. Li, and Z. Yang. Preparation of hydroxylated lecithin complexed iodine/-carboxymethyl chitosan/sodium alginate composite membrane by microwave drying and its applications in infected burn wound treatment. *Carbohydrate Polymers*, **206**:435–445, (2019).
DOI: https://doi.org/10.1016/j.carbpol.2018.10.068.

[62] A. Lee, A. Hudson, D. Shiwarski, J. Tashman, T. Hinton, S. Yerneni, J. Bliley, P. Campbell, and A. Feinberg. 3D bioprinting of collagen to rebuild components of the human heart. *Science*, **365**(6452):482–487, (2019).
DOI: https://doi.org/10.1126/science.aav9051.

[63] S. Murugesan and T. Scheibel. Chitosan-based nanocomposites for medical applications. . *Journal of Polymer Science*, **59**(15):1610–1642, (2021).
DOI: https://doi.org/10.1002/pol.20210251.

[64] L. Van Damme, P. Blondeel, and S. Van Vlierberghe. Injectable biomaterials as minimal invasive strategy towards soft tissue regeneration-an overview. *Journal of Physics: Materials*, **4**(2): 022001, (2021).
DOI: https://doi.org/10.1088/2515-7639/abd4f3.

[65] A. Habib, V. Sathish, S. Mallik, and B. Khoda. 3D printability of alginate-carboxymethyl cellulose hydrogel. *Materials*.

[66] J. Keating and M. McQueen. Substitutes for autologous bone graft in orthopaedic trauma. *Journal of Bone & Joint Surgery British*, **83** (1):3–8, (2001).
DOI: https://doi.org/10.1302/0301-620x.83b1.11952.

[67] Y.-F. Feng, L. Wang, X. Li, Z.-S. Ma, Y. Zhang, Z.-Y. Zhang, and W. Lei. Influence of architecture of β-tricalcium phosphate scaffolds on biological performance in repairing segmental bone defects. *PLoS One*, **7**(11):e49955, (2012).
DOI: https://doi.org/10.1371/journal.pone.0049955.

[68] S. B. Sulaiman, T. K. Keong, C. H. Cheng, A. B. Saim, and R. B. H. Idrus. Tricalcium phosphate/hydroxyapatite (TCP-HA) bone scaffold as potential candidate for the formation of tissue engineered bone. *Indian Journal of Medical Research*, **137**(6):1093–1101.

[69] Y. Zhang and M. Zhang. Synthesis and characterization of macroporous chitosan/calcium phosphate composite scaffolds for tissue engineering. *Journal of Biomedical Materials Research: An Official Journal of The Society for Biomaterials*, **55**(3):304–312, (2001).
DOI: https://doi.org/10.1002/1097-4636(20010605)55:3¡304::aid-jbm1018¿3.0.co;2-j.

[70] J. S. Boateng, A. D. Auffret, K. H. Matthews, M. J. Humphrey, H. N. Stevens, and G. M. Eccleston. Characterisation of freeze-dried wafers and solvent evaporated films as potential drug delivery systems to mucosal surfaces. *International Journal of Pharmaceutics*, **389**(1-2): 24–31, (2010).
DOI: https://doi.org/10.1016/j.ijpharm.2010.01.008.

[71] M. M. Kalani, J. Nourmohammadi, and B. Negahdari. Osteogenic potential of Rosuvastatin immobilized on silk fibroin nanofibers using argon plasma treatment. *Biomedical Materials*, **14**(2):025002, (2018).
DOI: https://doi.org/10.1088/1748-605X/aaec26.

[72] C. K. Min, U. M. Wikesjö, J. C. Park, G. J. Chae, S. D. Pippig, P. Bastone, C. S. Kim, and C. K. Kim. Wound healing/regeneration using recombinant human growth/differentiation factor-5 in an injectable poly-lactide-co-glycolide-acid composite carrier and a one-wall intrabony defect model in dogs. *Journal of Clinical Periodontology*, **38** (3):261–268, (2011).
DOI: https://doi.org/10.1111/j.1600-051X.2010.01691.x.

[73] B. L. Eppley, W. S. Pietrzak, and M. W. Blanton. Allograft and alloplastic bone substitutes: a review of science and technology for the craniomaxillofacial surgeon. *Journal of Craniofacial Surgery*, **16** (6):981–989, (2005).
DOI: https://doi.org/10.1097/01.scs.0000179662.38172.dd.

[74] P. Valerio, M. M. Pereira, A. M. Goes, and M. F. Leite. The effect of ionic products from bioactive glass dissolution on osteoblast proliferation and collagen production. . *Biomaterials*, **25**(15):2941–2948, (2004).
DOI: https://doi.org/10.1016/j.biomaterials.2003.09.086.

[75] O. Tsigkou, J. R. Jones, J. M. Polak, and M. M. Stevens. Differentiation of fetal osteoblasts and formation of mineralized bone nodules by 45S5 Bioglass® conditioned medium in the absence of osteogenic supplements. *Biomaterials*, **30**(21):3542–3550, (2009).
DOI: https://doi.org/10.1016/j.biomaterials.2009.03.019.